Journal of Biomaterials and Nanobiotechnology, **2014, 5, 24-30**
Published Online January 2014 (http://www.scirp.org/journal/jbnb)
http://dx.doi.org/10.4236/jbnb.2014.51004

Poly(Vinyl Alcohol)/Collagen/Hydroxyapatite Nanoparticles Hybrid System Containing Yttrium-90 as a Potential Agent to Treat Osteosarcoma

Marcelo F. Cipreste, Edesia M. B. Sousa

Serviço de Nanotecnologia e Materiais Nucleares, Centro de Desenvolvimento da Tecnologia Nuclear/Comissão Nacional de Energia Nuclear (CDTN/CNEN), Belo Horizonte, Brasil.
Email: sousaem@cdtn.br

Received November 4th, 2013; revised December 14th, 2013; accepted January 2nd, 2014

ABSTRACT

Osteosarcoma is the most common primary malignant bone tumors, affecting mostly children, adolescents and young adults. This is an aggressive tumor that results in a high mortality rate and poor prognosis. Due to the low sensitivity of osteosarcoma to ionizing radiation, such treatment is not used very often and it can be recommended only to postsurgical therapy. As an alternative therapy, functionalized nanomaterials allow their accumulation in tumor tissues due to their unique properties, making them good agents to act as stable carriers for radionuclides. In this work, mesoporous hydroxyapatite nanoparticles were synthesized and the functionalization process with poly(vinyl alcohol) and collagen was investigated. The samples were characterized by X-ray diffraction (XRD), N_2 adsorption, elemental analysis (CHN), Fourier Transform Infrared Spectroscopy (FTIR), Nitrogen Adsorption, Transmission Electron Microscopy (TEM), and Thermal Analysis. Also, the yttrium incorporation potential and its release kinetics in the hydroxyapatite matrix were evaluated to study the capacity of this system to treat osteosarcomas. The results indicate that this material has a promisor potential to treat this kind of tumor.

KEYWORDS

Osteosarcoma; Hydroxyapatite Nanoparticles; PVA; Collagen; Yttrium-90

1. Introduction

Osteosarcoma is the most common primary malignant bone tumors, affecting mostly children, adolescents and young adults [1]. The number of new cases of bone tumors up to 19 years is approximately estimated in 670 cases per million inhabitants per year in Brazil [2,3]. This is an aggressive tumor that results in a high mortality rate and poor prognosis [4]. A neoadjuvant chemotherapy followed by an invasive surgical resection is the most common treatment for this pathology. Due to the low sensitivity of osteosarcoma to ionizing radiation, such treatment is not used very often and it can be recommended only to postsurgical therapy [5-7]. Considering these difficulties, there is an emergent need to find new therapeutic alternatives.

Nanostructured systems have been widely exploited in biomedical research with great optimism for the diagnosis and therapy of cancer. Nanomaterials, such as mesoporous silica, hydroxyapatite nanoparticles, carbon nanotubes and liposomes, have unique properties that allow their accumulation in tumor tissues, making them good agents to act as carriers for controlled drug release or stable carriers for radionuclides [8].

Hydroxyapatite (HA) nanoparticles, chemically defined as $Ca_{10}(PO_4)_6(OH)_2$, have been extensively explored for biological applications due to excellent biocompatibility, bioactivity and similarity to the chemical composition of human bone tissue [9]. The small crystallite size of these nanomaterials is a very important factor

related to biological and structural properties, such as surface activity and low dissolution rate [10]. Also, the mesoporous structure of biomaterials allows the easy incorporation of agents, such as radioisotopes, aiming the treatment of pathologies such as osteosarcoma [11]. In addition, the literature show that functionalized HA nanoparticles present great binding rates on osteosarcoma lineages cells [12].

Bone tissue is an inorganic-bioorganic composite material consisting mainly of collagen (Col) and HA. It is related in the literature that the functionalization process of hydroxyapatite surfaces with collagen improves the adherence of this material on bone like tissues [12]. However, the synthesized biocomposites of collagen and hydroxyapatite alone do not have adequate mechanical properties for some biomedical applications. This behavior can be optimized by polymeric binders that provide improved durability and mechanical properties for these materials [13]. Poly(vinyl alcohol) (PVA) hydrogels exhibit biocompatibility and high elastic modulus, allowing the use of this polymer for several biomedical applications including drug delivery systems and radioisotope carries [14,15].

Yttrium-90 is a beta emitter radioisotope (E_{max} = 2.28 MeV) with a half-life of 64 h. This radionuclide has been widely studied as a potential agent for radiation synovectomy [16,17], and also showed a good stability for ^{90}Y-HA preparation for in vitro applications [17]. In addition, this radioisotope has been used in brachytherapy to treat metastatic liver tumors in microspheres labeled systems [18,19].

Although hydroxyapatite microparticles containing yttrium-90 had already been studied in some previous works [17,18], to the best of our knowledge, no works actually address the investigation of the use of functionalized nanostructured hydroxyapatite in nanometer scale as an yttrium-90 carrier system. The size range of the particles is a very important feature for cancer treatment materials. In inflammatory and hypoxia conditions, typically observed in tumor regions, the endothelial lining of the blood vessel wall becomes more permeable than in the normal state. As a result, large molecules and small particles ranging from 10 to 500 nm can leave the vascular system and accumulate within the interstitial tumor space [8]. The spontaneous accumulation, which works especially well with tumors due to the lack of lymphatic drainage, is known as enhanced permeability and retention (EPR) [8]. Within the pharmaceutical field, the synthetic polymers of vinyl series might protect particulate drug carriers from undesirable interactions with biological surrounded components [20], making them avoidable to the macrophages and becoming long-circulating materials, allowing them to accumulate in tumor tissues by EPR effect [8,20].

The combination of nanostructured materials carriers and radioisotopes presents a promising potential for the treatment of osteosarcoma allowing more selective use of radiation in tumor cells. This approach can increase the sensitivity of tumors to the radiation due to the possibility to maintain the nanostructured carrier between radioisotopes and tumor cells. In this sense the objective of this work is to synthesize a hybrid system of PVA/Col/HA mesoporous nanoparticles conjugated with yttrium and evaluates this system as a potential therapeutic agent for osteosarcoma.

2. Methods

2.1. Hydroxyapatite Production

Mesoporous hydroxyapatite nanoparticles were synthesized using the cationic surfactant method following the literature [21,22] with some modifications. The HA synthesis started with the preparation of two precursors solutions. Solution (1) was prepared by dissolving a preweighed amount of calcium nitrate, $Ca(NO_3)_2{\cdot}4H_2O$, in Milli-Q® water to obtain a 0.167 M of calcium concentration. Solution (2) was prepared by dissolving 2 g of cetyltrimethylammonium bromide (CTAB) in Milli-Q® water and adding a preweighed amount of dipotassium hydrogen phosphate, $K_2HPO_4{\cdot}3H_2O$, to obtain a 0.1 M of phosphate concentration. Solution (2) was stirred for 6 hours to promote a net assembly by micelles formation and its pH was adjusted to 12 with NaOH 2.5 M during the slowly drop-wise addiction of Solution (1). After the dropping process, the final solution was aged at room temperature during 14 hours. The resultant solution was conducted to a hydrothermal treatment at 100˚C during 10 hours. After, the solution was filtered, dried during 24 hours at 60˚C temperature and calcined during 6 hours at 550˚C to obtain a fine white powder.

2.2. HA/PVA/Col Functionalization

The functionalization of HA nanoparticles with PVA and collagen process was performed following the literature [13,14] with some modifications. A solution of 7.3 wt% PVA was prepared by dissolving pre-weighed amounts of PVA in Milli-Q® water at 90˚C during 6 hours with vigorous stirring. Then, 450 mg of HA was added to 30 mL of PVA solution and kept stirring at 60˚C during 4 hours. After, 600 mg of collagen was added to 20 mL of the HA/PVA solution and stirred at room temperature during 5 hours. The final solution was centrifuged and dried at 40˚C to preserve the collagen structure.

2.3. Yttrium Incorporation and Release Assays

Firstly, an aqueous solution of 1:1 (Y:HA/PVA/Col) was

prepared and kept stirring at 200 rpm at room temperature during 48 hours. The final solution was filtered using swinex system with a 100 nm pore membrane. The liquid (I.HA-Y) was analyzed by atomic emission spectrometry method with inductively coupled plasma (ICP-AES, Spectroflame—Spectro Analytical Instruments, Germany) to determinate the amount of yttrium incorporated on mesoporous HA nanoparticles. The powder was used to value the release kinetics assays during variable times (12, 24, 48, 72, 96 and 120 hours). Each solution was filtered using swinex system and analyzed by ICP-AES to value the amount of yttrium released from HA nanoparticles.

2.4. Yttrium Activation Potential

The yttrium activation potential by (n, γ) nuclear reaction of $^{89}YCl_3$ (131.9 mg) was calculated following the literature [23,24] for neutron activation on TRIGA IPR-R1 nuclear reactor sited on CDTN/CNEN, Belo Horizonte, Brazil. Equation (1) was feed with TRIGA reactor constants:

$$A = N\left(\phi_{Th}\sigma_{Th} + \phi_{EPI}I_{\gamma}\right)\left(1 - e^{-\lambda T_{IR}}\right) \quad (1)$$

where A is the activity, N is the number of target nuclei, ϕ_{Th} is the thermal neutron flux on central tube, σ_{Th} is the radionuclide thermal neutron cross section, ϕ_{EPI} is the epithermal neutron flux on central tube, I_{γ} is the radionuclide capture resonance integral, λ is the radionuclide decay constant (λ = ln2/$T_{1/2}$; $T_{1/2}$ is the radioisotope half-life) and T_{IR} is the irradiation time.

2.5. Characterizations

The crystalline phases of synthesized HA nanoparticles were evaluated by X-ray diffraction (XRD, Rigaku Inc., Japan) with CuKα radiation in which data were collected from 4˚ to 80˚ (2θ) with a step size of 4˚/min. Particles size analyses, morphology and porosity of mesoporous HA nanoparticles were evaluated by transmission electron microscopy (TEM, Tecnai G2-12 SpiritBiotwin—FEI Company, Japan). The surface parameters were evaluated by N_2 adsorption (Autosorb iQ—Quantachrome, EUA), the samples were outgassed for 2 hours at 300˚C and the specific surface area was calculated by the traditional method of Brunauer, Emmett and Teller (BET). Fourier transform infrared spectra (FTIR, ThermoScientific—Nicolet 6700, USA) were recorded in the range of 4000 - 400 cm^{-1} with 64 scans to evaluate the chemical composition of the samples. Thermogravimetric analyses (TGA, DTG-60H—Shimadzu, Japan) were carried out under nitrogen atmosphere from room temperature to 800 ˚C. CHN elemental analyses (CHN, 2400—PerkinElmer, USA) were performed to investigate the presence of PVA and collagen on functionalized samples.

3. Results and Discussion

3.1. X-Ray Diffraction

The powder XRD of the synthesized hydroxyapatite is shown on **Figure 1** which reveals a single phase formation of hexagonal HA with P63/m space group (JCPDS files: 09-0432) and no characteristic peaks of impurities are observed. This analysis points to a pure production of hydroxyapatite and indicates that the presence of CTAB cannot induce the crystallization of any other phases.

3.2. Transmission Electron Microscopy

In order to evaluate the mesoporous HA nanoparticles size, morphology and porosity, transmission electron microscopy was carried out as shown in **Figure 2**. The rod like morphology and porosity can be observed in accordance with results from literature [10,11]. As estimated by the Quantikov Image Analyzer data [25], the particles are monodisperse and present an average mean diameter of approximately 87 nm.

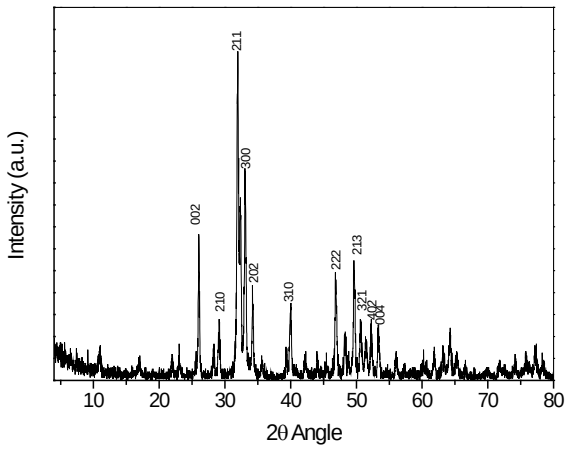

Figure 1. XRD pattern of the synthesized mesoporous hydroxyapatite nanoparticles.

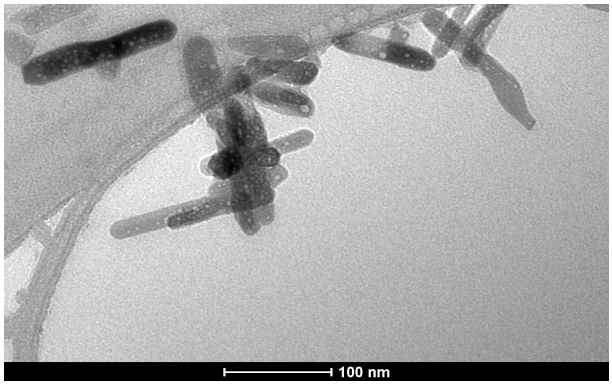

Figure 2. TEM image of mesoporous HA nanoparticles.

3.3. Nitrogen Adsorption Analysis

Nitrogen adsorption isotherm is shown on **Figure 3** and the surface parameters of HA nanoparticles determined by BET method are shown on **Table 1**. The HA porosity, previously determined by TEM analysis, was confirmed by BET results, indicating that mesoporous particles were produced with 17.5 nm of pore diameter and 0.086 cm^3/g of pore volume, allowing this material to be used as a radioisotope carrier. The specific surface area found as 56 m^2/g determines a great potential for functionalization processes.

3.4. Fourier Transform Infrared Spectroscopy

The FTIR studies were performed to investigate the chemical composition of the samples. **Figure 4(c)** shows FTIR spectrum of the HA nanoparticles in agreement with the literature [10,11,13]. All the stretching and bending vibrations of the PO_4^{3-} and OH^- functional groups of hydroxyapatite could be observed. The weak shoulder at 960 cm^{-1} and strong broad band around 1035 cm^{-1} corresponds to v_1 and v_3 phosphate stretching modes while the shoulder at 473 cm^{-1} and the strong peaks at 568 and 604 cm^{-1} points the presence of v_2 and v_4 phosphate bending modes [11]. The OH^- bands could be observed at 3576 and 634 [10]. The broad band observed from 3237 to 3663 cm^{-1} could be attributed to H_2O vibration modes.

The success of functionalization process was evaluated by comparing FTIR spectra of pure PVA, pure collagen, pure HA and HA/PVA/Col hybrid system as shown on **Figures 4-6**. The collagen spectrum (**Figure 4(b)**) shows absorption bands of amine I (C=O) at 1660 cm^{-1} and amine II and III groups at 1449, 1388 and 1239 cm^{-1}. The 1529 cm^{-1} peak is associated with the C-N stretching of amines I and II [13]. **Figure 4(a)** shows the presence of absorption peaks at 869, 663 and 420 cm^{-1} for PVA. Comparing the scale-expanded FTIR spectrum of pure col and PVA with PVA/Col/HA material (**Figures 5** and **6**), it can be observed that some characteristic stretching and bending vibrations present in the PVA and col spectra are observed in the PVA/Col/HA FTIR spectrum in lower intensities. However, we did not observe all characteristic vibrations of the functionalizing groups, because some vibration modes of pure PVA and pure collagen occurred in the same frequency interval of the HA modes (**Figure 4**).

3.5. Thermogravimetric Analyses

Thermogravimetric analyses were performed to investigate the chemical changes during heat treatment of the synthesized mesoporous hydroxyapatite nanoparticles and to investigate the success of the functionalization process with PVA and collagen. **Figure 7** shows the TGA and DTG plots for pure HA, PVA/HA and PVA/Col/HA hybrid systems. There is no significant weight losses for pure HA nanoparticles, suggesting that a thermal stable material was synthesized with great agreement with literature [11]. The weight loss observed up to 250˚C may be attributed to the thermodesorption of physically adsorbed water. Comparing the TGA and DTG plots for PVA/HA and PVA/Col/HA systems, it is possible to visualize weight losses corresponding to PVA and collagen degradations in temperatures ranging around 200˚C to 450˚C. Also, it is possible to infer that these losses are due to the presence of both PVA and collagen in the HA nanoparticle matrix, in agreement with the FTIR analyses, en-

Table 1. Isotherm BET results for HA nanoparticles.

Surface parameters		
Specific surface area (m^2/g)	*Porous diameter* (nm)	*Pore volume* (cm^3/g)
56	17.5	0.086

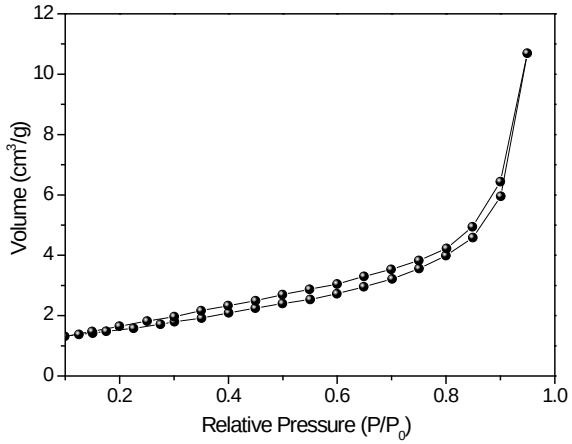

Figure 3. Nitrogen adsorption isotherm of the synthesized mesoporous hydroxyapatite nanoparticles.

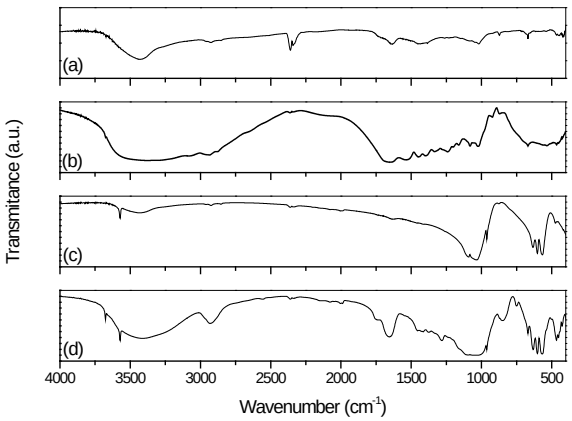

Figure 4. FTIR Spectra for (a) pure PVA, (b) pure collagem, (c) pure HA and (d) HA/PVA/Col hybrid system.

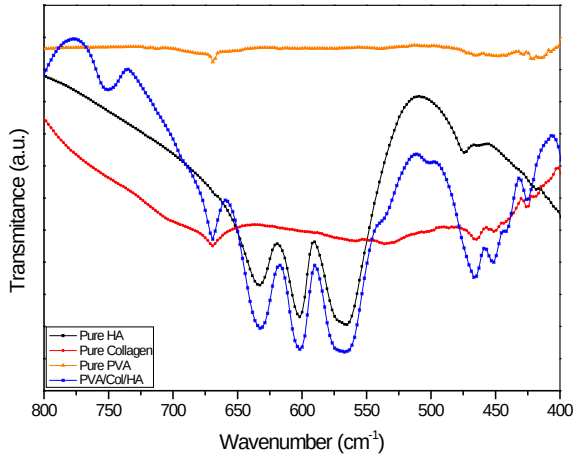

Figure 5. Selective range of FTIR spectra showing matching peaks of the systems from 400 to 800 cm^{-1}.

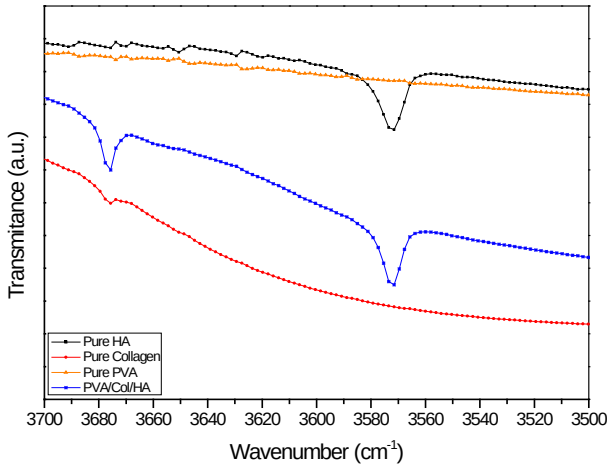

Figure 6. Selective range of FTIR spectra showing matching peaks of the systems from 3500 to 3700 cm^{-1}.

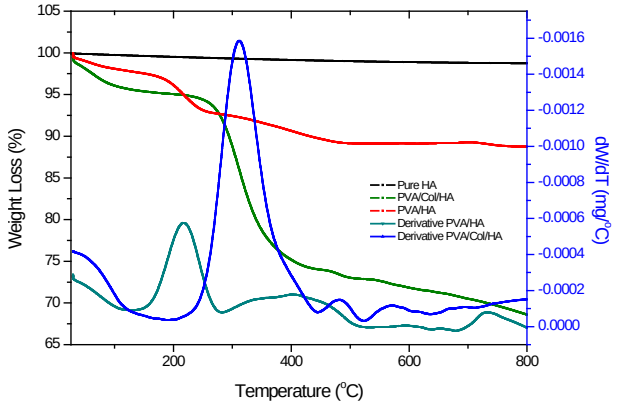

Figure 7. TGA plots for pure HA, PVA/HA system and PVA/Col/HA hybrid system. DTG plots for PVA/HA and PVA/Col/HA.

forcing that a successful functionalization process was reached.

3.6. CHN Elemental Analyses

The presence of PVA and collagen on the functionalized mesoporous HA nanoparticles was also evaluated by CHN elemental analysis which is shown on Table 2. The functionalized samples presented higher carbon concentrations in both PVA and PVA/Col samples, as compared to the HA nanoparticle matrix, confirming the presence of anchored functionalized agents on its surfaces. The CHN results for PVA/HA sample shows smaller amounts of carbon, hydrogen and nitrogen when compared to PVA/Col/HA sample, indicating that HA nanoparticles was functionalized with both PVA and collagen materials.

3.7. Yttrium Incorporation and Release Assays

Table 3 shows the ICP-AES results of yttrium content and release assays. A capacity of adsorption around 32% of yttrium element in PVA/Col/HA matrix can be evaluated from these results, aiming to a concentration of 24 wt% of this element in HA nanoparticles. ICP-AES results also show that no significant yttrium amount can be released from PVA/Col/HA matrix.

3.8. Theoretical Evaluation of Yttrium Activation

Table 4 summaries the Equation (1) variable values for TRIGA reactor [23,24] and shows the theoretical calcu-

Table 2. CHN elemental analysis results.

Element	Samples		
	Pure HA	PVA/HA	PVA/Col/HA
C	0%	2.161%	8.708%
H	0%	0.497%	1.482%
N	0%	0%	0.822%

Table 3. Yttrium incorporation and release assays.

Samples	ICP-AES readings for yttrium concentrations on supernatants (mg/L)
I.HA-Y	5100 ± 500
R.HA-Y 12 h	<0.20[a]
R.HA-Y 24 h	<0.20[a]
R.HA-Y 48 h	<0.20[a]
R.HA-Y 72 h	<0.20[a]
R.HA-Y 96 h	<0.20[a]
R.HA-Y 120 h	<0.20[a]

[a]Limit of detection = 0.20 mg/L.

Table 4. Equation (1) variable values and calculated activity.

Variable	*Values*
A	130.8 MBq
N	4.1E20
Φ_{TH}	2.8E12 n·cm^{-1}·s^{-1}
σ_{TH}	1.28E-24 cm^2
Φ_{EPI}	2.6E11 n·cm^{-1}·s^{-1}
I_γ	1E-24 cm^2
$T_{1/2}$	64 h
T_{IR}	8 h

lated activity of 130.8 MBq for 60 mg of yttrium-89 activation (45.5% of 131.9 mg of $^{89}YCl_3$). This value indicates that this system presents a potential as nanoplatform for cancer treatment. Data presented in this work show that Y^{90}PVA/Col/HA have adequate characteristic to be used in *in vitro* cell culture studies to determine the cytotoxicity of this sample in UMR-6 cell line. These experiments will be conducted and reported in the due course.

4. Conclusion

The characterization results confirm the success of the nanoparticles synthesis in accordance with the expected. The data indicate that the functionalized nanostructures were prepared with adequate characteristic for *in vivo* applications, showing great yttrium incorporation potential as well as very low release kinetics. These are promisor results for a radioisotope carrier material, considering that a great radioactivity with no radionuclide losses can be associated with this matrix. In view of all results obtained, the system can be considered as a potential therapeutic alternative for the treatment of osteosarcoma.

REFERENCES

[1] J. C. Wittig, J. Bickels, D. Priebat, J. Jelinek, K. Kellar-Graney, B. Shmookler and M. M. Malawer, "Osteosarcoma: A Multidisciplinary Approach to Diagnosis and Treatment," *American Family Physician*, Vol. 65, No. 6, 2002, pp. 1123-1132.

[2] C. T. Fundato, A. S. Petrilli, C. G. Dias and M. G. R. de Gutiérrez, "Itinerário Terapêutico de Adolescentes e Adultos Jovens com Osteossarcoma," *Revista Brasileira de Cancerologia*, Vol. 58, No. 2, 2012, pp. 197-208.

[3] B. de Camargo, M. de Oliveira Santos, M. S. Rebelo, R. de Souza Reis, S. Ferman, C. P. Noronha and M. S. Pombo-de-Oliveira, "Cancer Incidence among Children and Adolescents in Brazil: First Report of 14 Population-Based Cancer Registries," *International Journal of Cancer*, Vol. 126, No. 3, 2010, pp. 715-720. http://dx.doi.org/10.1002/ijc.24799

[4] Z. Shi, X. Huang, B. Liu, H. Tao, Y. Cai and R. Tang, "Biological Response of Osteosarcoma Cells to Size-Controlled Nanostructured Hydroxyapatite," *Journal of Biomaterials Applications*, Vol. 25, No. 1, 2010, pp. 19-37. http://dx.doi.org/10.1177/0885328209339396

[5] W. S. Ferguson and A. M. Goorin, "Current Treatment of Osteosarcoma," *Cancer Investigation*, Vol. 19, No. 3, 2001, pp. 292-315. http://dx.doi.org/10.1081/CNV-100102557

[6] D. Carrle and S. S. Bielack, "Current Strategies of Chemotherapy in Osteosarcoma," *International Orthopaedics*, Vol. 30, No. 6, 2006, pp. 445-451. http://dx.doi.org/10.1007/s00264-006-0192-x

[7] K. Ando, M. F. Heymann, V. Stresing, K. Mori, F. Redini and D. Heymann, "Current Therapeutic Strategies and Novel Approaches in Osteosarcoma," *Cancers* (*Basel*), Vol. 5, No. 2, 2013, pp. 591-616. http://dx.doi.org/10.3390/cancers5020591

[8] V. Torchilin, "Tumor Delivery of Macromolecular Drugs Based on the EPR Effect," *Advanced Drug Delivery Reviews*, Vol. 63, No. 3, 2011, pp. 131-135. http://dx.doi.org/10.1016/j.addr.2010.03.011

[9] Y. J. Han, S. C. J. Loo, N. T. Phung, H. T. Ong, S. J. Russell, K.-W. Peng, F. Boey and J. Ma, "Controlled Size and Morphology of EDTMP-Doped Hydroxyapatite Nanoparticles as Model for 153Samarium-EDTMP Doping," *Journal of Materials Science*: *Materials in Medicine*, Vol. 19, No. 9, 2008, pp. 2993-3003. http://dx.doi.org/10.1007/s10856-008-3426-1

[10] M. Mir, F. L. Leite, P. S. de P. Herrmann Jr., F. L. Pissetti, A. M. Rossi, E. L. Moreira and Y. P. Mascarenhas, "XRD, AFM, IR and TGA Study of Nanostructured Hydroxyapatite," *Materials Research Bulletin*, Vol. 15, No. 4, 2012, pp. 622-627. http://dx.doi.org/10.1590/S1516-14392012005000069

[11] G. Verma, K. C. Barick, N. Manoj, A. K. Sahu and P. A. Hassan, "Rod-Like Micelle Templated Synthesis of Porous Hydroxyapatite," *Ceramics International*, Vol. 39, No. 8, 2013, pp. 8995-9002. http://dx.doi.org/10.1016/j.ceramint.2013.04.100

[12] S. Vohra, K. M. Hennessy, A. A. Sawyer, Y. Zhuo and S. L. Bellis, "Comparison of Mesenchymal Stem Cell and Osteosarcoma Cell Adhesion to Hydroxyapatite," *Journal of Materials Science*: *Materials in Medicine*, Vol. 19, No. 12, 2008, pp. 3567-3574. http://dx.doi.org/10.1007/s10856-008-3525-z

[13] N. Degirmenbasi, D. M. Kalyon and E. Birinci, "Biocomposites of Nanohydroxyapatite with Collagen and Poly(Vinyl Alcohol)," *Colloids Surfaces B Biointerfaces*, Vol. 48, No. 1, 2006, pp. 42-49. http://dx.doi.org/10.1016/j.colsurfb.2006.01.002

[14] W. Song, D. C. Markel, X. Jin, T. Shi and W. Ren, "Poly(Vinyl Alcohol)/Collagen/Hydroxyapatite Hydrogel: Properties and *in Vitro* Cellular Response," *Journal of Biomedical Materials Research Part A*, Vol. 100, No. 11,

2012, pp. 3071-3079.
http://dx.doi.org/10.1002/jbm.a.34240

[15] N. A. Peppas and N. K. Mongia, "Ultrapure Poly (Viny1 Alcohol) Hydrogels with Mucoadhesive Delivery Characteristics," Vol. 43, 1997, pp. 51-58.

[16] U. Pandey, A. Mukherjee, P. R. Chaudhary, M. R. Pillai and M. Venkates, "Preparation and Studies with 90Y-Labelled Particles for Use in Radiation Synovectomy," *Applied Radiation and Isotopes*, Vol. 55, No. 4, 2001, pp. 471-475.

[17] M. Khalid and A. Mushtaq, "Preparation and *in Vitro* Stability of (n,Gamma) Yttrium-90 Hydroxyapatite," *Applied Radiation and Isotopes*, Vol. 62, No. 4, 2005, pp. 587-590. http://dx.doi.org/10.1016/j.apradiso.2004.08.046

[18] O. N. Kucuk, C. Soydal, S. Lacin, E. Ozkan and S. Bilgic, "Selective Intraarterial Radionuclide Therapy with Yttrium-90 (Y-90) Microspheres for Unresectable Primary and Metastatic Liver Tumors," *World Journal of Surgical Oncology*, Vol. 9, No. 1, 2011, p. 86.
http://dx.doi.org/10.1186/1477-7819-9-86

[19] J. Metyko, J. M. Williford, W. Erwin, J. Poston and S. Jimenez, "Long-Lived Impurities of 90Y-Labeled Microspheres, Thera-Sphere and SIR-Spheres, and the Impact on Patient Dose and Waste Management," *Health Physics*, Vol. 103, No. 5 Suppl. 3, 2012, pp. S204-S208.
http://dx.doi.org/10.1097/HP.0b013e31826566f0

[20] V. P. Torchilin and V. S. Trubetskoy, "Which Polymers Can Make Nanoparticulate Drug Carriers Long-Circulating?" *Advanced Drug Delivery Reviews*, Vol. 16, No. 2-3, 1995, pp. 141-155.
http://dx.doi.org/10.1016/0169-409X(95)00022-Y

[21] X. Wu, X. Song, D. Li, J. Liu, P. Zhang and X. Chen, "Preparation of Mesoporous Nano-Hydroxyapatite Using a Surfactant Template Method for Protein Delivery," *Journal of Bionic Engineering*, Vol. 9, No. 2, 2012, pp. 224-233.
http://dx.doi.org/10.1016/S1672-6529(11)60105-4

[22] M. Khalid, M. Mujahid, S. Amin, R. S. Rawat, A. Nusair and G. R. Deen, "Effect of Surfactant and Heat Treatment on Morphology, Surface Area and Crystallinity in Hydroxyapatite Nanocrystals," *Ceramics International*, Vol. 39, No. 1, 2013, pp. 39-50.
http://dx.doi.org/10.1016/j.ceramint.2012.05.090

[23] M. Â. B. C. Menezes and R. Jaćimović, "Optimised k0-Instrumental Neutron Activation Method Using the TRIGA MARK I IPR-R1 Reactor at CDTN/CNEN, Belo Horizonte, Brazil," *Nuclear Instruments and Methods in Physics Research A*, Vol. 564, No. 2, 2006, pp. 707-715.
http://dx.doi.org/10.1016/j.nima.2006.04.013

[24] D. M. Zangirolami, "Thermal and Epithermal Neutron Fluence Rates in the Irradiation Facilities of the TRIGA IPR-R1 Nuclear Reactor," *Brazilian Journal of Physics*, Vol. 40, No. 1, 2010, pp. 47-51.

[25] L. C. M. Pinto, "Quantikov: Um Analisador Microestrutural Para o Ambiente Windows," Ph.D. Thesis, Instituto de Pesquisas Energéticas e Nucleares (IPEN), São Paulo, 1996.